Research Journal of Applies Sciences, Engineering and Technology 5(2): 519-530, 2013
DOI:10.19026/rjaset.5.4984
ISSN: 2040-7459; E-ISSN: 2040-7467

Submitted: May 13, 2012 Accepted: May 29, 2012 Published: January 11, 2013

Research Article

Effects of Radiation and Heat Generation/Absorption on MHD Free Convective Heat Transfer of Power-Law Non-Newtonian Fluids Along a Power-Law Stretching Sheet with Uniform Surface Heat Flux

M.A. Samad and M.R. Hossain
Department of Mathematics, University of Dhaka, Dhaka-1000, Bangladesh

Abstract: An analysis is carried out to investigate the effects of MHD free convection heat transfer of power-law non-Newtonian fluids along a stretching sheet. This has been done under the simultaneous action of suction, heat generation/absorption, thermal radiation and uniform transverse magnetic field. The stretching sheet is assumed to continuously moving with a power-law velocity and maintaining a uniform surface heat flux. The governing nonlinear partial differential equations are transformed into a system of nonlinear ordinary differential equations using appropriate similarity transformations. The resulting non-linear equations are solved numerically using Nachtsheim-Swigert shooting iterative technique along with sixth order Runge-Kutta integration scheme. Numerical results for the non-dimensional velocity and temperature profiles are shown graphically and discussed. The effects of skin-friction coefficient and the local Nusselt number which are of physical and engineering interest are studied and presented graphically as well as in the form of tables for the variation of different physically important parameters. A comparison of the present study is also performed with the previously published study and found excellent agreement.

Keywords: Boundary layer, dilatant fluid, heat transfer, magnetic field, pseudo-plastic fluid, suction

INTRODUCTION

The study of MHD flow of an electrically conducting fluid on heated stretching sheet becomes an important matter due to its many engineering and physical applications in modern metallurgical and metal-working process. Hot rolling, drawings of plastic films and artificial fibers, glass fiber production, metal extrusion, crystal growing, petrochemical industry, heat exchange design are examples of such physical applications. Sakiadis (1961) first presented boundary layer flow over a continuous solid surface moving with constant speed. Elbashbeshy (1998) investigated heat transfer over a stretching surface with variable and uniform surface heat flux subject to injection and suction. Vajravelu and Hadjinicolaou (1997) studied the convective heat transfer in an electrically conducting fluid near an isothermal stretching sheet and they studied the effect of internal heat generation or absorption.

The study of non-Newtonian fluid flow and heat transfer over a stretched surface gets attention due to its numerous applications industrially. These types of fluid exhibit non linear relationship between shear stress and rate of strain such as polymer solutions, molten plastics, pulps, paints and foods. Rajgopal *et al*. (1984) studied flow of viscoelastic fluid over stretching sheet. Dandapat and Gupta (1989) extended the problem to study heat transfer and Datti *et al*. (2005) analyzed the problem over a non-isothermal stretching sheet. The MHD boundary layer flow over a continuously moving plate for a micropolar fluid has been studied by Raptis (1998) and Rahman and Sattar (2006). Several authors (Anderson *et al*., 1992; Mahmoud and Mahmoud, 2006) adopted the non-linearity relation as power-law dependency of shear stress on rate of strain. Recently, Chen (2008) studied the effect of magnetic field and suction/injection on the flow of power-law non-Newtonian fluid over a power-law stretched sheet subject to a surface heat flux.

All the above investigations are restricted to MHD flow and heat transfer problems. However, of late, the radiation effect on MHD flow and heat transfer problems has become more important industrially. Many processes in engineering areas occur at high temperatures and the knowledge of radiative heat transfer becomes very important for the design of the pertinent equipments. Nuclear power plants, gas turbines and the various propulsion devices for aircrafts, missiles, satellites and space vehicles are examples of such engineering areas. The interaction of radiation with hydromagnetic flow has become industrially more prominent in the processes wherever high temperatures occur. Takhar *et al*. (1996) analyzed the radiation effects on MHD free convection flow past a semi-infinite vertical plate using Runge-Kutta Merson

Corresponding Author: M.R. Hossain, Department of Mathematics, University of Dhaka, Dhaka-1000, Bangladesh

quadrature. Chamkha (2001) analyzed radiation effects on free convection flow past a semi-infinite vertical plate. Raptis and Perdikis (1999) studied radiation and free convection flow past a moving plate.

In this present study, we have investigated the effect on MHD free convective heat transfer of power-law non-Newtonian fluids along a continuously moving stretching sheet in the presence of radiation and heat generation/absorption with uniform surface heat flux. The present study is a more generalized form of the previous study performed by Chen (2008). In this study we have considered the effects of free convection, radiation and heat generation/absorption which were not considered in the work of Chen (2008). We also compare this study to the previous study and found excellent agreement.

METHODOLOGY

Governing equations: Let us consider a steady two dimensional MHD free convection laminar boundary layer flow of a viscous incompressible and electrically conducting fluid obeying the power-law model along a permeable stretching sheet under the influence of thermal radiation and heat generation/absorption. Introducing the Cartesian coordinate system, the X-axis is taken along the stretching sheet in the vertically upward direction and the Y-axis is taken as the normal to the sheet. Two equal and opposite forces are introduced along the X-axis, so that the sheet is stretched. This continuous sheet is assumed to move with a velocity according to a power-law form, i.e., $u_w = Cx^p$ and be subject to a uniform surface heat flux. We also consider the ambient temperature of the flow as T_∞. The fluid is considered to be gray, absorbing-emitting radiation but non-scattering medium and the Rosseland approximation is used to describe the radiative heat flux in the energy equation. The radiative heat flux in the X-direction is considered negligible in comparison to the Y-direction. A strong magnetic field is applied in the Y-direction. Here, we can neglect the effect of the induced magnetic field in comparison to the applied magnetic field. The electrical current flowing in the fluid gives rise to an induced magnetic field if the fluid were an electrical insulator,but here we have taken the fluid to be the electrically conducting. Hence, only the applied magnetic field B plays a role which gives rise to magnetic forces in the X-direction. We also bring into account of temperature dependent volumetric heat generation q^m, in the region that is given by Vajravelu and Hadjinicolaou. (1997) as:

$$q^m = \begin{cases} Q_0(T - T_\infty), T \geq T_\infty \\ 0, T \leq T_\infty \end{cases} \quad (1)$$

where, Q_0 is the heat generation/absorption constant. Under the above assumptions, the governing boundary layer equations are:

$$\frac{\partial u}{\partial x} + \frac{\partial v}{\partial y} = 0 \quad (2)$$

$$u\frac{\partial u}{\partial x} + v\frac{\partial u}{\partial y} = \frac{K}{\rho}\left(\left|\frac{\partial u}{\partial y}\right|^{n-1}\frac{\partial u}{\partial y}\right) + g\beta(T - T_\infty) - \frac{\sigma B^2 u}{\rho} \quad (3)$$

$$u\frac{\partial T}{\partial x} + v\frac{\partial T}{\partial y} = \alpha\frac{\partial^2 T}{\partial y^2} + \frac{Q_0}{\rho c_p}(T - T_\infty) - \frac{1}{\rho c_p}\frac{\partial q_r}{\partial y} \quad (4)$$

The radiative heat flux q_r is described by the Rosseland approximation (Rohsenow, 1998) such that:

$$q_r = -\frac{4\sigma_1}{3k_1}\frac{\partial T^4}{\partial y} \quad (5)$$

where,
σ_1 : The Stefan-Boltzman constant
k_1 : The Rosseland mean absorption coefficient

It is assumed that the temperature difference within the flow is sufficiently small such that T^4 can be expressed in a Taylor series about the free steam temperature T_∞ and then neglecting higher-order terms we obtain the following approximation:

$$T^4 \approx 4T_\infty{}^3 - 3T_\infty{}^4 \quad (6)$$

Using (5) and (6) in the last term of Eq. (4), we obtain:

$$\frac{\partial q_r}{\partial y} = -\frac{16\sigma_1 T_\infty^3}{3\rho c_p k_1}\frac{\partial^2 T}{\partial y^2} \quad (7)$$

Thus introducing q_r in Eq. (4), we obtain the governing equations in the following form:

$$\frac{\partial u}{\partial x} + \frac{\partial v}{\partial y} = 0 \quad (8)$$

$$u\frac{\partial u}{\partial x} + v\frac{\partial u}{\partial y} = \frac{K}{\rho}\left(\left|\frac{\partial u}{\partial y}\right|^{n-1}\frac{\partial u}{\partial y}\right) + g\beta(T - T_\infty) - \frac{\sigma B^2 u}{\rho} \quad (9)$$

$$u\frac{\partial T}{\partial x} + v\frac{\partial T}{\partial y} = \alpha\frac{\partial^2 T}{\partial y^2} + \frac{Q_0}{\rho c_p}(T - T_\infty) + \frac{16\sigma_1 T_\infty^3}{3\rho c_p k_1}\frac{\partial^2 T}{\partial y^2} \quad (10)$$

The appropriate boundary conditions are:

$$\left.\begin{array}{c} u_w = Cx^p, v = v_w, \partial T/\partial y = -q_w/k \text{ at } y = 0, x > 0 \\ u_w \to 0, T \to T_\infty \text{ as } y \to \infty \end{array}\right\} \quad (11)$$

where,

u and v : The velocity components
K : The consistency coefficient
c_p : The specific heat at constant pressure
$B(x)$: The magnetic field
T : The temperature of the field
g : The acceleration due to gravity
β : The volumetric coefficient of thermal expansion
σ : The electric conductivity
ρ : The density of the fluid
α : The thermal diffusivity
k : The thermal conductivity of the fluid
n : The flow behavior index
q_r : The radiative heat flux
q_w : Surface heat flux

Power index p: Surface is accelerated or decelerated for positive and negative values

The velocity component v_w at the wall having positive value to indicate suction and negative value for injection

Similarity analysis: In order to obtain a similarity solution of the problem, we introduce a similarity parameter $\delta(x)$ such that $\delta(x)$ is a length scale. We now introduce the following dimensionless variables (Chen, 2008):

$$\eta = \frac{y}{\delta(x)} = \left(\frac{C^{2-n}}{K/\rho}\right)^{1/(n+1)} x^{\frac{\{p(2-n)-1\}}{(n+1)}} y \quad (12)$$

$$\psi = \left(\frac{C^{1-2n}}{K/\rho}\right)^{-1/(n+1)} x^{\frac{\{p(2n-1)+1\}}{(n+1)}} f(\eta) \quad (13)$$

$$\phi(\eta) = \frac{(T-T_\infty) Re_x^{1/(n+1)}}{q_w x/k} \quad (14)$$

where,

ψ : The stream function
η : The dimensionless distance normal to the sheet
f : The dimensionless stream function
ϕ : The dimensionless fluid temperature, Then:

$$u = u_w f'$$

$$v = -u_w Re_x^{-\frac{1}{n+1}} \left(\frac{p(2n-1)+1}{n+1} f + \frac{p(2-n)}{n+1} \eta f'\right)$$

Using the transformations (12) to (14) in Eq. (9) and (10), we obtain the following dimensionless equations as:

$$\left(|f''|^{n-1} f''\right)' + \frac{p(2n-1)+1}{(n+1)} f f'' - p(f')^2 - M f' + \lambda\phi = 0 \quad (15)$$

$$\frac{3N+4}{3NPr}\phi'' + \frac{p(2n-1)+1}{(n+1)} f\phi' + \frac{p(2-n)-1}{(n+1)} f'\phi + Q\phi = 0 \quad (16)$$

The boundary conditions after transformation become:

$$\left.\begin{array}{c} f' = 1, f = \frac{n+1}{p(2n-1)+1} f_w, \phi' = -1 \text{ at } \eta = 0 \\ f' = 0, \phi = 0 \text{ as } \eta \to \infty \end{array}\right\} \quad (17)$$

where,

$M = \frac{\sigma B^2 x}{\rho u_w}$: The magnetic field parameter
$Pr = \frac{x u_w}{\alpha} Re_x^{-2/(n+1)}$: The generalized Prandtl number
$N = \frac{k k_1}{4\sigma_1 T_\infty^3}$: The radiation number
$f_w = -\frac{v_w}{u_w} Re_x^{1/(n+1)}$: The suction parameter
$Q = \frac{Q_0 x}{\rho u_w c_p}$: The heat source parameter
$\lambda = \frac{Gr}{Re_x^{1/(n+1)}} = \frac{g\beta(q_w/k)x^2}{u_w^2} Re_x^{\frac{-1}{(n+1)}}$: The buoyancy parameter
$Re_x = \frac{\rho u_w^{2-n} x^n}{K}$: The local Reynolds number

Here, we note that the magnetic field strength B should be proportional to x to the power of $(p-1)/2$ to eliminate the dependence of M on x, i.e., $B(x) = B_0 x^{(p-1)/2}$, where B_0 is a constant. The parameters of engineering interest for the present problem are skin friction coefficient (C_f) and local Nusselt number (Nu_x), which indicate physically wall shear stress and local wall heat transfer rate respectively. The skin friction coefficient (C_f) is given by:

$$C_f = \frac{\tau_w}{\frac{1}{2}\rho u_w^2} \quad \text{or,}$$

$$Re_x^{1/(n+1)} C_f = 2\,|f''(0)|^{n-1} f''(0) \quad (18)$$

and the local Nusselt number Nu_x is defined as:

$$Nu_x = \frac{hx}{k} = \frac{Re_x^{1/(n+1)}}{\phi(0)} \quad \text{or,}$$

$$Nu_x Re_x^{-1/(n+1)} = 1/\phi(0) \quad (19)$$

Thus from Eq. (18) and (19), we see that the skin friction coefficient C_f and local Nusselt number Nu_x are proportional to $2|f''(0)|^{n-1} f''(0)$ and $1/\phi(0)$, respectively.

RESULTS AND DISCUSSION

The system of transformed governing Eq. (15)-(16) with boundary conditions (17) is solved numerically

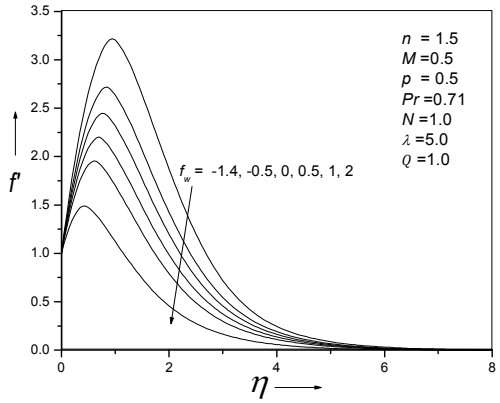

Fig. 1: Effect of suction parameter (f_w) on velocity profiles

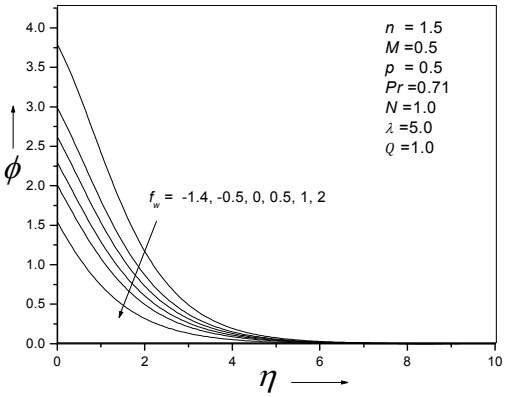

Fig. 2: Effect of suction parameter (f_w) on temperaturep rofiles

using Nachtsheim and Swigert (1965) shooting iterative technique along with sixth order Runge- Kutta integration scheme. Now in order to discuss the results, we solve the system (15)-(16) for different physically important parameters and carry out the discussion how these parameters do effect on the velocity and temperature of the flow field.

The effect of the suction/injection on the velocity and temperature field is shown in Fig. 1 and 2, respectively. We observe that the velocity profiles decrease with the increase of suction and the reverse trend is found for injection. It indicates the fact that for a fluid of higher suction, the velocity of the flow stabilizes very quickly (Fig. 1). The temperature profiles in Fig. 2 show that the temperature decreases with the increase of suction parameter (f_w).

The buoyancy force arises in free convective flows where the dependency of velocity field on temperature field exists. Figure 3 shows the effect on the velocity field, as velocity profiles increase with the increase of the buoyancy parameter (λ). The velocity increases quite rapidly for higher values of λ and stabilizes very quickly. Near $\eta = 2.5$ there is a cross flow to

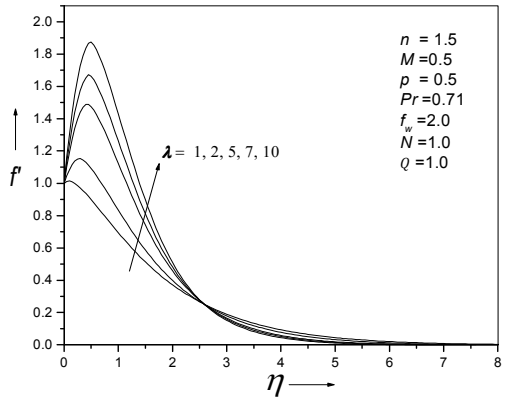

Fig. 3: Velocity profiles for different values of buoyancy parameter (λ)

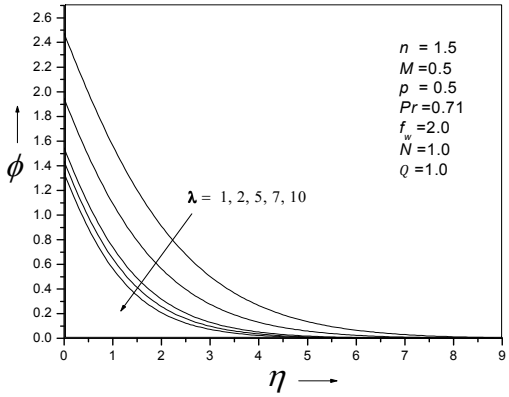

Fig. 4: Temperature profiles for different values of buoyancy parameter (λ)

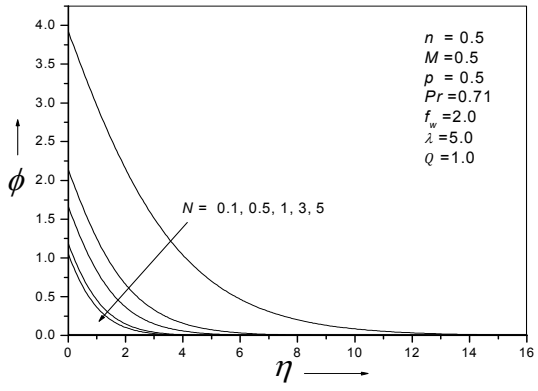

Fig. 5: Temperature profiles for different values of radiation number (N)

indicate the fact that, for smaller values of λ, velocity stabilizes rather slowly. On the other hand, Fig. 4 shows that the temperature profiles decrease as the buoyancy parameter (λ) increases.

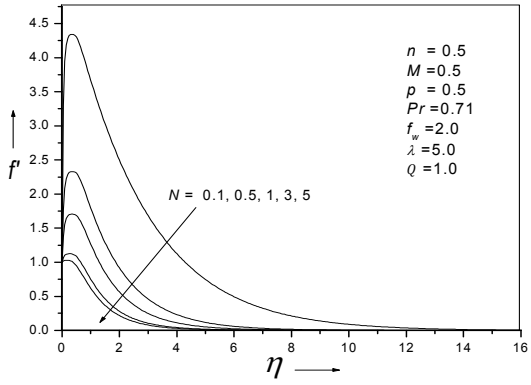

Fig. 6: Velocity profiles for different values of radiation number (N)

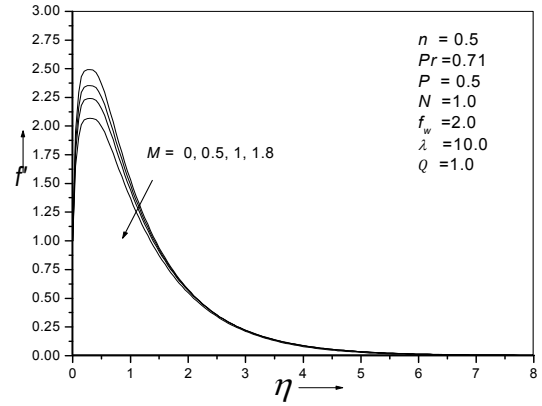

Fig. 7: Effect of magnetic parameter (M) on velocity profiles for n = 0.5

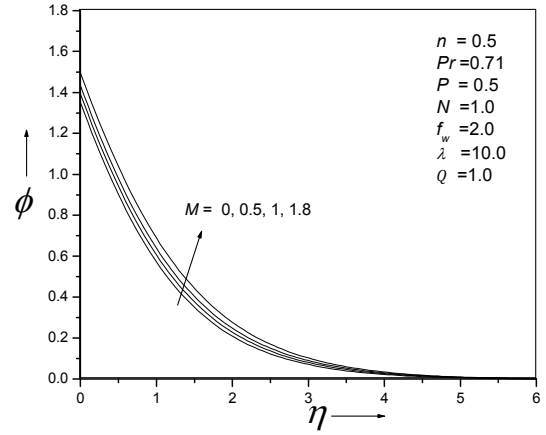

Fig. 8: Effect of magnetic parameter (M) on temperature profiles for n = 0.5

Due to the thermal radiation, the wall temperature decreases to a great extent. From Fig. 5, we find that, our umerical results agree with this experimental

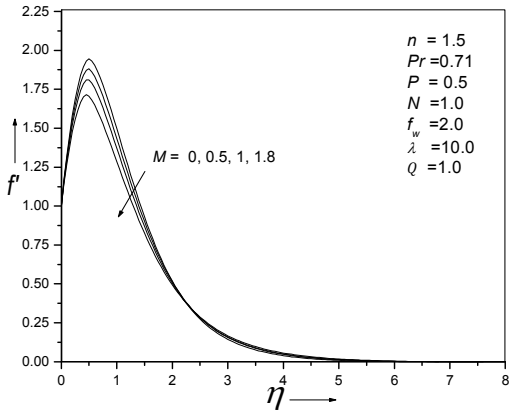

Fig. 9: Effect of magnetic parameter (M) on velocity profiles for n = 1.5

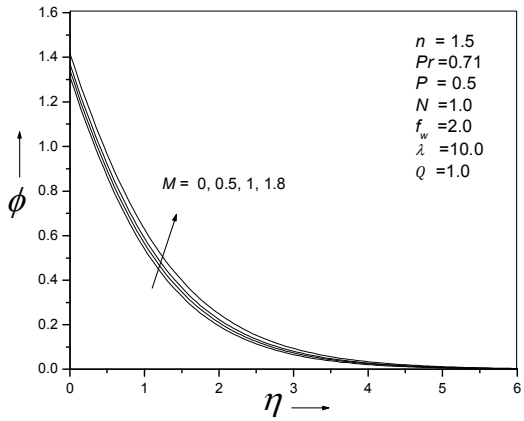

Fig. 10: Effect of magnetic parameter (M) on temperature profiles for n = 1.5

phenomenon. According to the Newton's law of cooling, the rate of heat transfer is thus increased. It is quite clear from the Fig. 5 and 6 that velocity and temperature profiles decrease as the radiation parameter (N) increases. The velocity profiles and wall temperature decrease very rapidly for $N \geq 1.0$ to indicate that the radiation effect can be used efficiently to control the velocity and temperature of the boundary layer.

It is observed from Fig. 7 to 10 that the velocity profiles decrease whereas temperature profiles increase as magnetic number (M) increases. However, from Fig. 7 and 9, it can be seen that there is a sharp rise in velocity profiles near the surface. Magnetic field lines act as strings to retard the motion. The consequence of which is to increase wall temperature. The effect of magnetic parameter (M) on temperature profiles is more noticeable for the pseudo-plastic fluids $(n < 1)$ than the dilatant fluids $(n > 1)$. Comparing Fig. 7 and

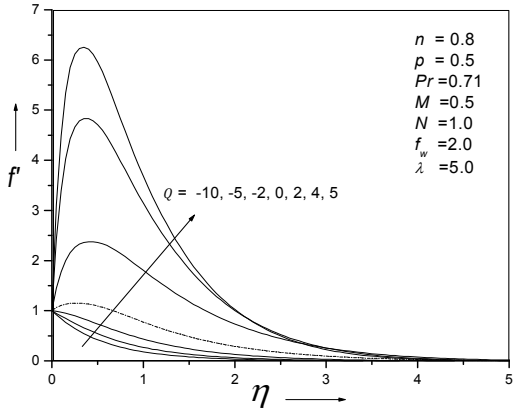

Fig. 11: Velocity profiles for different values of heat source parameter (Q)

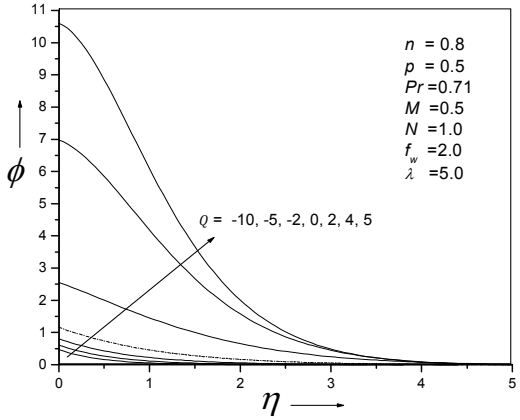

Fig. 12: Temperature profiles for different values of heat source parameter (Q)

9 we find that, the peaks of the velocity profiles for pseudo-plastics are higher than the dilatant fluids.

We found the effect of heat generation/absorption on velocity and temperature field from Fig. 11 and 12, respectively. We see that, both the velocity and temperature profiles increase due to heat generation. The dotted line represents the case without any external heat generation/absorption. The lines below the dotted line in both the figures correspond to heat absorption (negative values of Q). From Fig. 11 and 12 we see that, there is a sharp rise for $Q = 2.0, 4.0$ and 5.0 first near the surface, overshoot and then stabilizes rapidly. We also observe from Fig. 12 that the initial wall temperature is very high due to the heat generation and correspondingly the heat transfer rate is very small. Therefore, the heat transfer rate can be increased by absorbing heat from the surface of the stretched sheet.

Since the initial temperature gradient is negative, the temperature field stabilizes monotonically. We observe form Fig. 13 and 14 that, velocity and

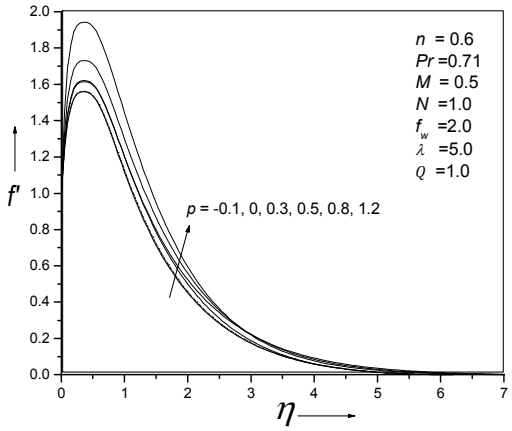

Fig. 13: Effect of velocity index (p) on velocity profiles for pseudo-plastic fluid (n<1)

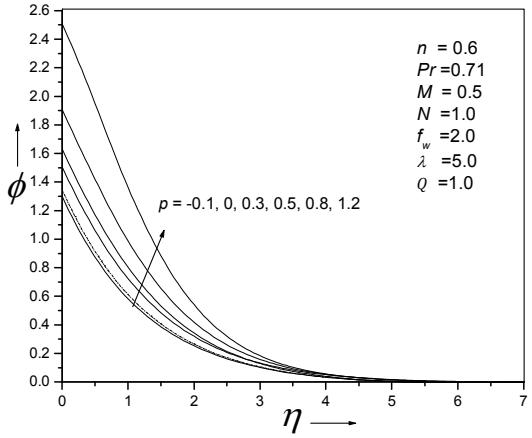

Fig. 14: Effect of velocity index (p) on temperature profiles for pseudo-plastic (n<1)

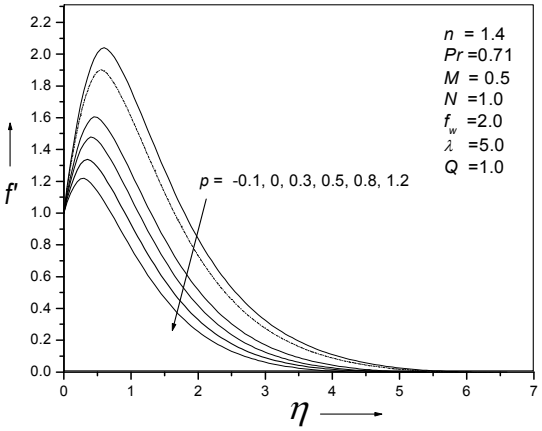

Fig. 15: Effect of velocity index (p) on velocity profiles for dilatant fluid (n>1)

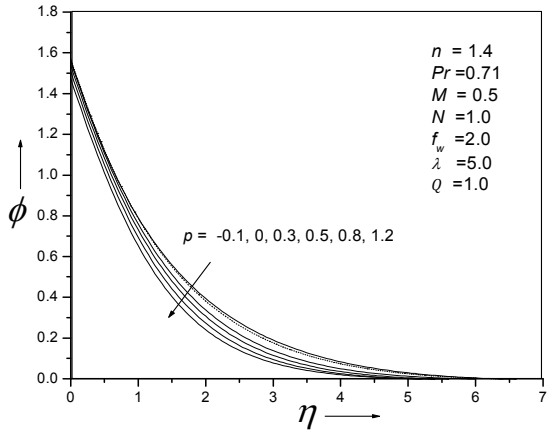

Fig. 16: Effect of velocity index (p) on temperature profiles for dilatant fluid (n>1)

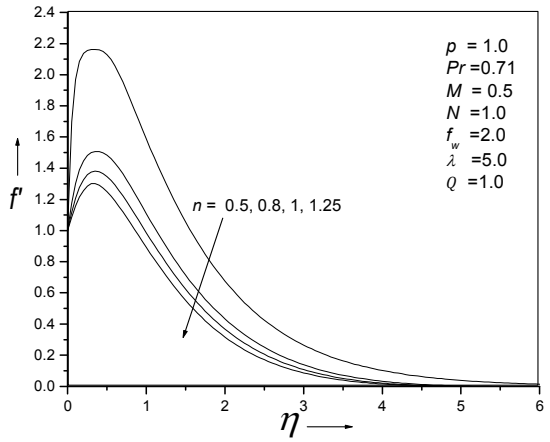

Fig. 17: Effect of power-law fluid index (n) on velocity profile for accelerated flow (p = 1.0)

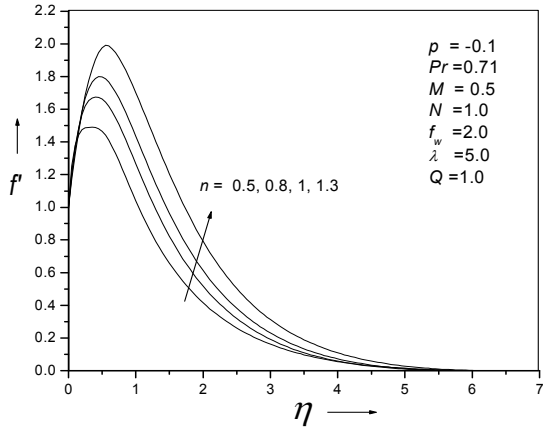

Fig. 18: Effect of power-law fluid index (n) on velocity profiles for decelerated flow (p = -0.1)

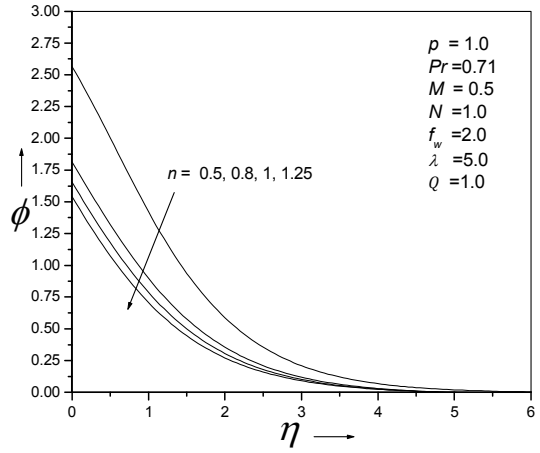

Fig. 19: Effect of power-law fluid index (n) on temperature profiles for accelerated flow (p = 1)

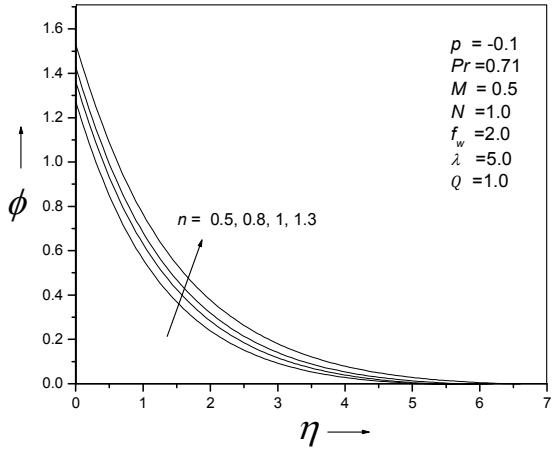

Fig. 20: Effect of power-law fluid index (n) on temperature profiles for decelerated flow (p = -0.1)

temperature increase with velocity index (p) for pseudo-plastic see that the effect of velocity index (p) on temperature profiles is more prominent in case of pseudo-plastics while the effect on velocity field is found to be prominent for dilatants (Fig. 15 and 16). The dotted line represents the flow along a surface of constant velocity $(p = 0)$.

Figure 17 illustrates that the velocity profiles decrease with the increase of power-law fluid index (n) for flows where the surface is accelerated $(p = 1)$.

However, the opposite trend velocity profiles for accelerated flow (p = 1) is quite clear for decelerated surface$(p = -0.1)$ flows from Fig. 18. The temperature profiles decrease with power-law fluid index (n) for $p = 1$ and increase for $p = -0.1$. Comparing Fig. 19 and 20, we find that the effect of power-law fluid index (n) on temperature profiles is more noticeable in case of accelerated surface flows.

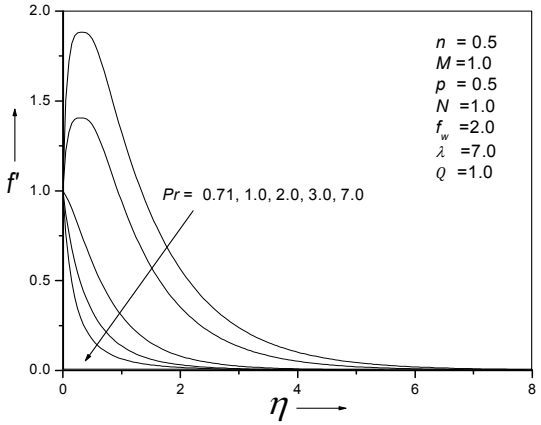

Fig. 21: Velocity profiles for different values of Prandtl number (Pr)

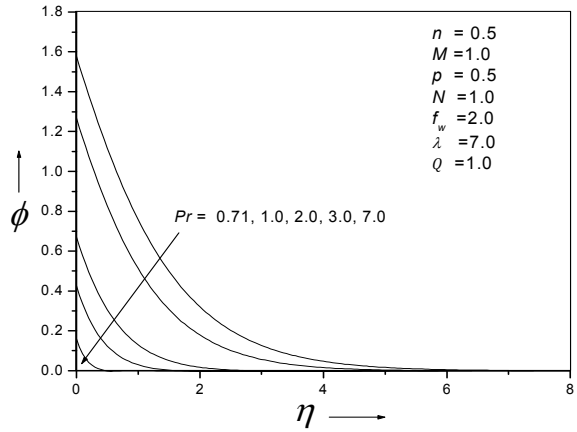

Fig. 22: Temperature profiles for different values of Prandtl number (Pr)

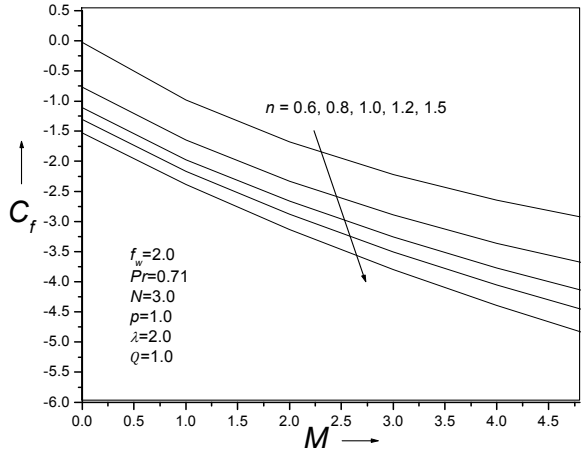

Fig. 23: Variation of C_f as a function of M at selected values of n

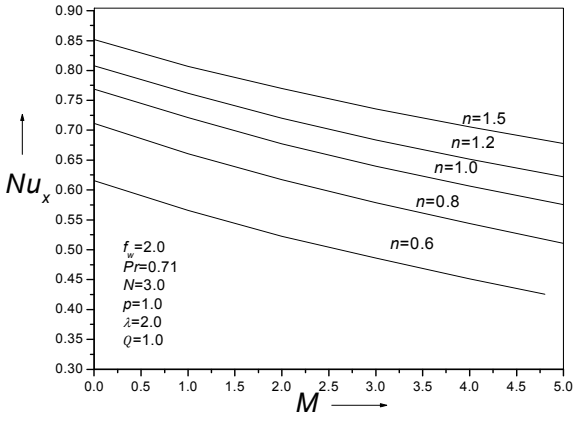

Fig. 24: Variation of Nu_x as a function of M at selected values of n

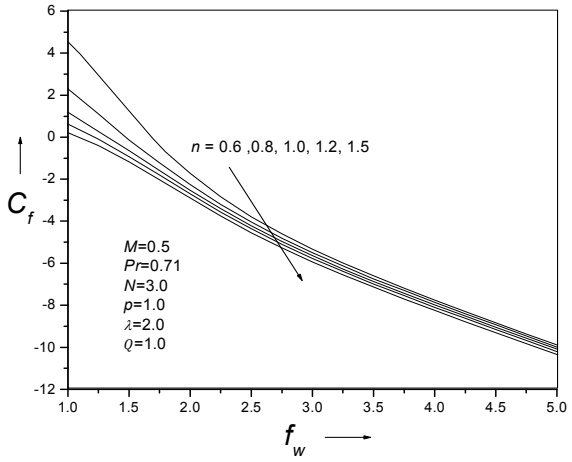

Fig. 25: Variation of C_f as a function of f_w at selected values of n

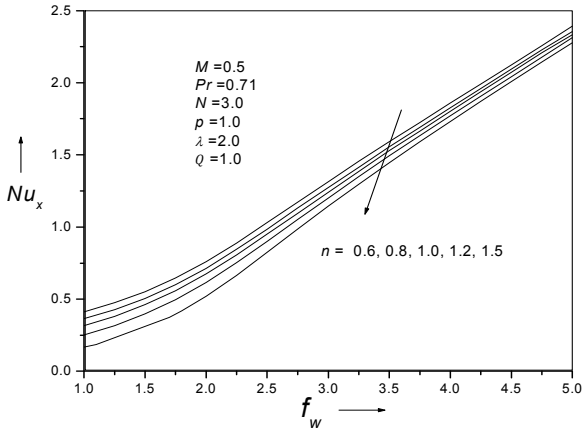

Fig. 26: Variation of Nu_x as a function of f_w at selected values of n

Figure 21 and 22 display the effect of Prandtl number (Pr) on velocity and temperature respectively. From both the figures we observe that the velocity and temperature profiles decrease with the increase of Prandtl number (Pr). The Prandtl number (Pr) represents the effective ratio of viscous diffusion rate and thermal diffusion rate. For $Pr = 0.71$ and 1.0, there is a rise in the velocity profiles near the stretching sheet. From Fig. 22 we see that for small Pr, the wall temperature is very high compared to larger values of Pr. For large Prandtl number, the wall temperature is very small and so the rate of heat transfer is very large (e.g., for petroleum oils and lubricants). Conveniently if $Pr >> 1$, then momentum boundary layer is thicker than thermal boundary layer. The opposite behavior can be visible for $Pr << 1$.

Figure 23 and 24 show the effect of Magnetic parameter (M) on the skin friction coefficient C_f and local Nusselt number Nu_x for various values of power-law fluid index (n). The skin friction coefficient C_f decreases with the increase of Magnetic parameter (M) and power-law fluid index (n). The local Nusselt number Nu_x also decreases for the increase of M. Here, it is clear from the Fig. 24 that Nu_x is larger for dilatant fluids $(n > 1)$ compared to pseudo-plastic fluids $(n < 1)$.

We observe from Fig. 25 and 26 that the skin friction coefficient C_f decreases with the increase of suction parameter (f_w). As the power-law index (n) increases, the skin friction coefficient C_f decreases with suction parameter (f_w). From Fig. 25 we observe that for small values of f_w, the skin friction coefficient C_f differs significantly with the change of power-law fluid index (n). The Nusselt number Nu_x , on the other hand increases Prandtl number (Pr) with the increase of f_w and decreases for the increase of power-law fluid index (n).

The effect of surface velocity index (p) on the skin friction coefficient C_f and local Nusselt number Nu_x has shown in Fig. 27 and 28 respectively. We see that the coefficient C_f decreases as the velocity index (p) increases. It is interesting to note that for smaller values of p, C_f increases with the increase of n, while the opposite behavior is visible for larger p. The local heat transfer rate on the other hand increases with n for negative and small positive values of p. The trend is reversed for a larger p.

Figure 29 and 30 display the effect of Prandtl number (Pr) on the skin friction coefficient C_f and local Nusselt number Nu_x. The skin friction coefficient C_f decreases with Prandtl number (Pr) for fixed n and p. For accelerated surface $(p = 0.5)$, C_f decreases with n. The effect of Prandtl number (Pr) on the skin friction coefficient C_f for pseudo-plastics, dilatants and Newtonian fluids are quite similar and coincide after

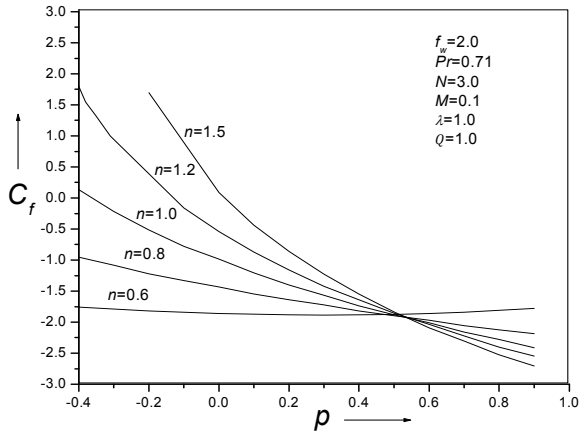

Fig. 27: Variation of C_f as a function of p at selected values of n

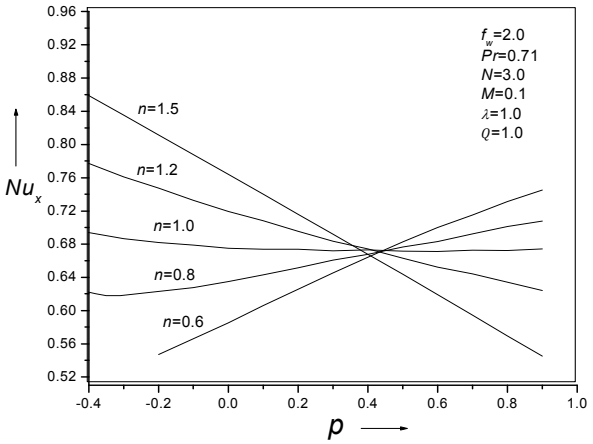

Fig. 28: Variation of Nu_x as a function of p at selected values of n

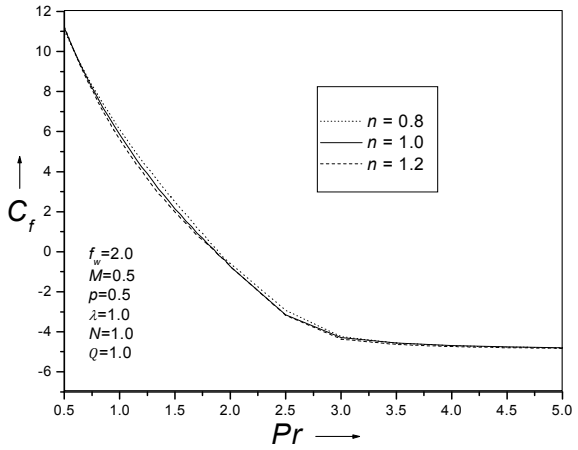

Fig. 29: Effect of Prandtl number (Pr) on skin friction coefficient

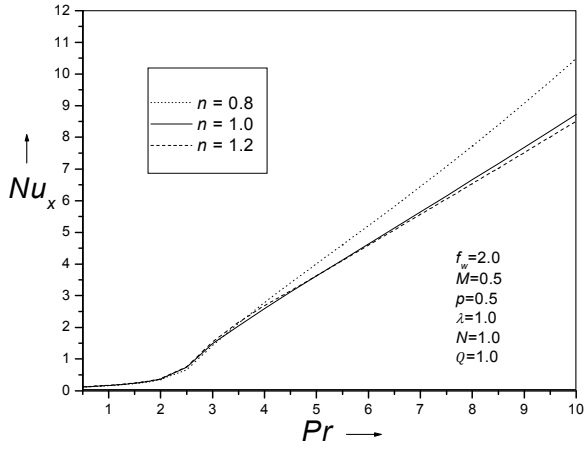

Fig. 30: Effect of Prandtl number (Pr) on local nusselt number

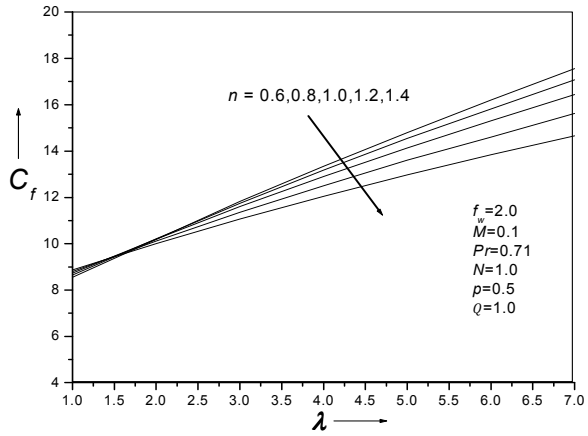

Fig. 31: Variation of C_f as a function of λ at selected values of n

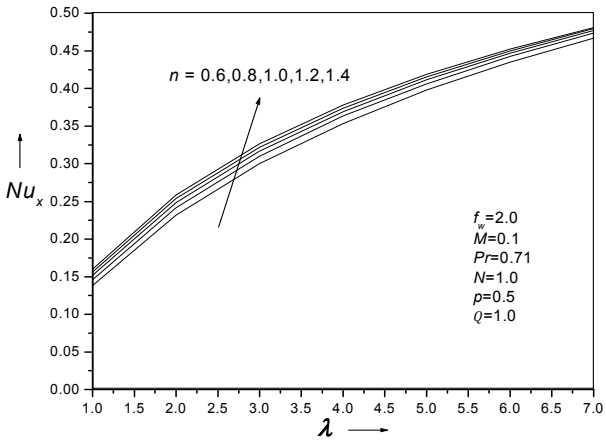

Fig. 32: Variation of Nu_x as a function of λ at selected values of n

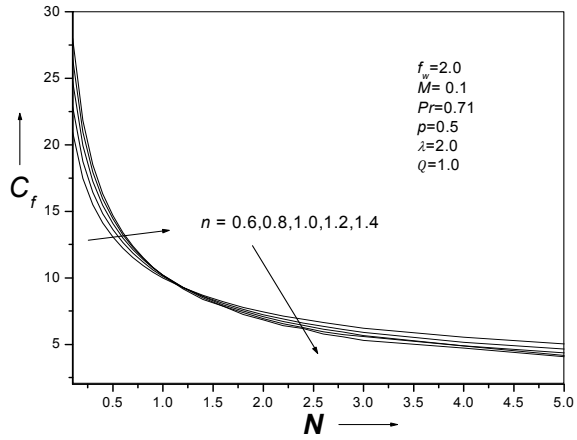

Fig. 33: Effect of radiation parameter (N) on skin friction coefficient

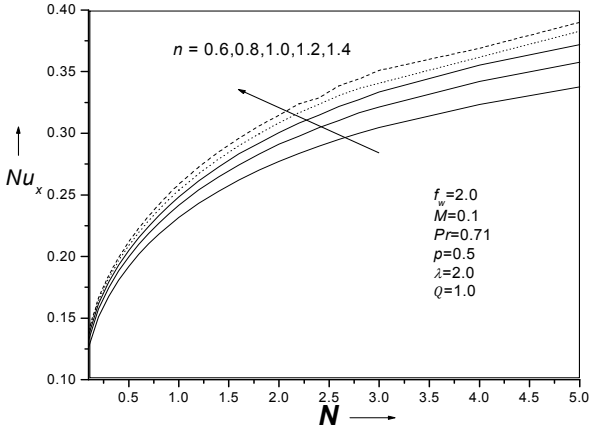

Fig. 34: Effect of radiation parameter (N) on local nusselt number

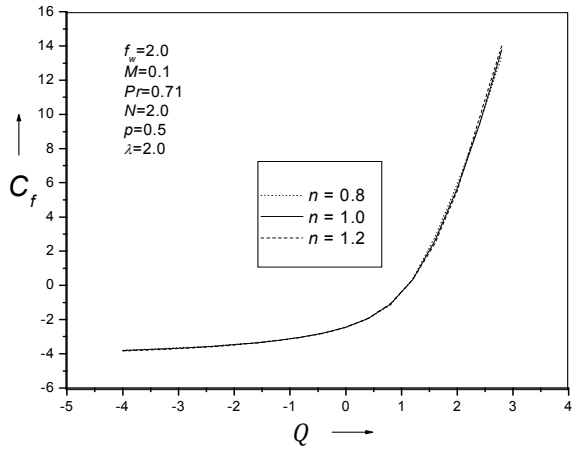

Fig. 35: Variation of C_f as a function of Q at selected values of n

Table 1: Comparison of skin friction coefficient and local nusselt number in the absence of radiation and heat generation/absorption of a forced convective flow (N = Q = λ = 0) for different values of n, M and f_w with Pr = 5 .0 and p = 0.5

			$-\mathrm{Re_x}^{1/(n+1)}\mathrm{C_f}$		$\mathrm{Nu_x}\mathrm{Re_x}^{-1/(n+1)}$	
n	M	f_w	Chen (2008)	Present study	Chen (2008)	Present study
0.5	1	0.0	2.633241	2.6334386	1.346116	1.3461035
		0.6	3.213067	3.2137484	3.683003	3.6833107
	5	0.6	4.608094	4.6078741	3.528467	3.5287845
1.0	1	0.0	2.519363	2.5193782	1.578424	1.5785883
		0.6	3.198565	3.1985827	3.866662	3.8672224
	5	0.0	4.726210	4.7262298	1.320497	1.3231287
		0.6	5.366930	5.3668243	3.754876	3.7553935
1.5	1	0.0	2.412287	2.4121919	1.689593	1.6902300
		0.6	3.178401	3.1782320	3.958697	3.9593387
	5	0.6	5.768535	5.7687145	3.874307	3.8749347
1.9	1	0.0	2.349473	2.3491838	1.744168	1.7481880
		0.6	3.170979	3.1709705	4.005932	4.0067115

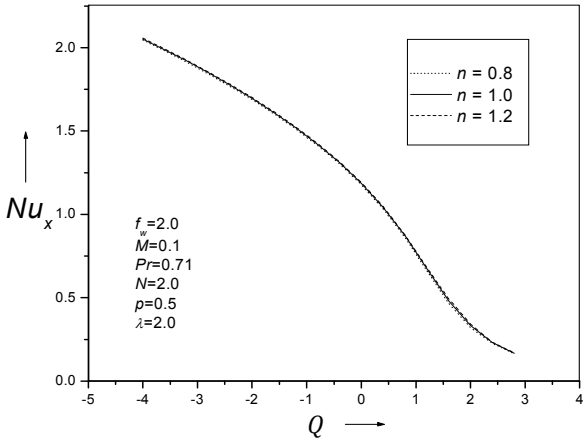

Fig. 36: Variation of Nu_x as a function of Q at selected values of n

$Pr = 2.8$. The effect of Prandtl number (Pr) on heat transfer rate has shown for the range $0.5 \leq Pr \leq 10$ in the Fig. 30.

From the Fig. 31 and 32 we find that, the skin friction coefficient C_f increases with buoyancy parameter (λ) and the effect of buoyant force is more noticeable for smaller power-law fluid index (n). The effect of buoyancy parameter (λ) on the heat transfer rate is very small, although it decreases the wall temperature. The heat transfer rate increases for increasing buoyancy parameter (λ) and with the flow behavior index (n).

Figure 33 and 34 reveal the effect of radiation number (N) on skin friction coefficient C_f and local Nusselt number Nu_x for different values of power-law fluid index (n). Due to radiation the wall temperature decreases and consequently the heat transfer rate increases. This effect is more prominent for larger power-law fluid index (n), shown in Fig. 34. The skin friction coefficient C_f decreases with radiation number (N). Also, C_f decreases with the flow behavior index (N). Also, C_f decreases with the flow behavior index n for $N \geq 1.0$ and increases for $N \leq 1.0$ and thus we have a cross flow (Fig. 33). For a fixed value of n, C_f decreases very rapidly for $0 < N \leq 1$.

The effect of heat source parameter (Q) on skin friction coefficient C_f and local Nusselt number Nu_x are shown in the Fig. 35 and 36. The negative values of Q corresponds to heat absorption (heat sink), where the thermal energy is absorbed by surroundings and thus cooling the surface. From Fig. 35 and 36 we observe that the skin friction coefficient C_f increases while local Nusselt number Nu_x decreases with the increase of heat source parameter (Q).

The effect of heat source parameter (Q) on different values of flow behavior index (n) is found to be negligible as the lines corresponds to $n = 0.8, n = 1.0$ and $n = 1.2$ coincide in both the figures (Fig. 35 and 36) with $Pr = 0.71$, $M = 0.1$, $N = 2.0$, $p = 0.5$ and $f_w = 2.0$.

Code verification and comparison: To assess the accuracy of our code, we calculated the skin friction coefficient and the local heat transfer rate. We compared these physically important parameters with Chen (2008) for forced convection (i.e., $\lambda = 0$) and found excellent agreement (Table 1).

CONCLUSION

From the present investigation we can make the following conclusions:

- Thermal radiation can be used effectively to control the velocity and thermal boundary layers
- Suction stabilizes boundary layer growth
- The buoyancy force increases the wall friction and thus thickening the velocity boundary layer

- The heat transfer rate can be increased by absorbing thermal energy from the surface
- Drag of the pseudo-plastics along a stretched surface decreases as the velocity index increases
- A strong magnetic field can be applied to increase the wall temperature of the pseudo-plastic fluids
- The heat transfer rate of dilatant fluids are greater than pseudo-plastic fluids for a decelerated surface flow while the opposite behavior is visible for accelerated surface flow

REFERENCES

Anderson, H.I., K.H. Bech and B.S. Dandapat, 1992. Magnetohydrodynamic flow of a power-law fluid over a stretching sheet. Int. J. Non-Linear Mech., 27: 926-936.

Chamkha, A.J., H.S. Takhar and V.M. Soundalgekar, 2001. Radiation effects on free convection flow past a semi-Infinite vertical plate with mass transfer. Chem. Eng. J., 84: 335-342.

Chen, C.H., 2008. Effects of magnetic field and suction/injection on convective heat transfer on non-Newtonian power-law fluids past a power-law stretched sheet with surface heat flux. Int. J. Thermal Sci., 47: 954-961.

Dandapat, B.S. and A.S. Gupta, 1989. Flow and heat transfer in a viscoelastic fluid over a stretching sheet. Int. J. Non-Linear Mech., 24: 215-219.

Datti, P.S., K.V. Prasad, M.S. Abel and A. Joshi, 2005. MHD viscoelastic fluid flow over a non-isothermal stretching sheet. Int. J. Eng. Sci., 42: 935-946.

Elbashbeshy, E.M.A., 1998. Heat transfer over a stretching surface with variable surface heat flux. J. Phys. D Appl. Phys., 31: 1951-1954.

Mahmoud, M.A.A. and M.A.E. Mahmoud, 2006. Analytical solutions of hydromagnetic boundary layer flow of non-Newtonian power-law fluid past a continuously moving surface. Acta Mech., 181: 83-89.

Nachtsheim, P.R. and P. Swigert, 1965. Satisfaction of the asymptotic boundary conditions in numerical solution of the system of nonlinear equations of boundary layer type. NASA TND-3004.

Rahman, M.M. and M.A. Sattar, 2006. Magnetohydrodynamic convective flow of a micropolar fluid past a continuously moving vertical porous plate in the presence of heat generation/absorption. ASME J. Heat Transf., 128: 142-152.

Rajgopal, K.R., T.Y. Na and A.S. Gupta, 1984. Flow of a viscoelastic fluid over a stretching sheet. Rheol. Acta, 23: 213-215.

Raptis, A., 1998. Flow of a micropolar fluid past a continuously moving plate by the presence of radiation. Int. J. Heat Mass Transf., 41: 2865-2866.

Raptis, A. and C. Perdikis, 1999. Radiation and free convection flow past a moving plate. Appl. Mech. Eng., 4: 817-821.

Rohsenow, W.M., J.P. Hartnett and Y.I. Cho, 1998. Handbook of Heat Transfer. 3rd Edn., McGraw-Hill, New York, pp: 1344, ISBN: 0070535558,

Sakiadis, B.C., 1961. Boundary layer behavior on Contiuous solid surface: I the boundary layer equations for two dimensional and axissym--metric flow. AICHE J., 7: 26-28.

Takhar, H.S., R.S.R. Gorla and V.M. Soundalgekar, 1996. Radiation effects on MHD free conve--ction flow of a radiating fluid past a semi-infinite vertical plate. Int. J. Num. Methods Heat Fluid Flow, 6: 77-83.

Vajravelu, K. and A. Hadjinicolaou, 1997. Convective heat transfer in an electrically conducting fluid at a stretching surface with uniform free stream. Internat. J. Engrg. Sci., 35(12-13): 1237-1244.